

# Protein Diffusion in Porous Chromatographic Media Studied by Proton and Fluorine PFG-NMR

Jonathan L. Coffman,<sup>\*,†</sup> Edwin N. Lightfoot, and Thatcher W. Root

Department of Chemical Engineering, University of Wisconsin, 1415 Johnson Drive, Madison, Wisconsin 53706

Received: August 21, 1996; In Final Form: November 26, 1996<sup>⊗</sup>

Diffusivities of several proteins or protein variants in nonadsorbing rigid-polymer and bonded-phase-silica chromatographic media were determined using pulsed-field-gradient NMR of both proton and fluorine nuclei. Solute size, pore size, and concentration all affect the intraparticle diffusivity. The intraparticle diffusivity of proteins is well represented by a hindered diffusion of a sphere in a long cylinder and a tortuosity factor of 2.0 for a ratio of solute diameter to pore diameter ranging from 0 to 0.3. An investigation of the effects of fluorine labeling on protein chemistry and hydrodynamics revealed that the extensive fluorine labeling denatured the protein, increasing its effective Stokes radius. The fluorine labeling did not, however, significantly alter the intraparticle diffusivity variation dependence on protein and pore sizes.

## 1. Introduction

Understanding diffusion in porous media is important for many industrial and biological applications. It is currently an active area for both theoretical and experimental research. In particular, diffusion of proteins in chromatographic media is important to quantify because it dominates mass transport in well-packed columns at conventional flow rates, as well as mass transport in “perfusive” systems at high flow rates. Quantifying the protein diffusivity is important to describe accurately chromatographic behavior during scale-up.

There currently exists no well-accepted theory for predicting diffusion of proteins in a rigid porous medium. The hydrodynamic theory relating the free solution diffusivity to that in straight long cylinders or slits has been extensively reviewed.<sup>1,2</sup> The hydrodynamic hindrance of pore walls on the protein mobility is represented<sup>2</sup> by a factor  $K_D$  typically less than or equal to unity. This hydrodynamic factor is typically cast as a function of  $\lambda = r_s/R_{\text{pore}}$ , the ratio of the solute Stokes radius,  $r_s$  (Table 1), to that of the pore radius  $R_{\text{pore}}$  (Table 2).

The effect of tortuosity in the absence of this hydrodynamic hindrance is often represented<sup>3</sup> by a single tortuosity factor  $\kappa$ . The expected values for the tortuosity factor  $\kappa$  are between 1 and 6,<sup>4–10</sup> with more extreme values possible for systems with anisotropy on the length scale studied.<sup>8,11</sup> A tortuosity factor of 2 is expected for an isotropic porous medium.<sup>3</sup>

Since diffusion in a porous medium potentially has contributions from both hydrodynamic hindrance and tortuosity, they are often lumped together into a single factor relating intraparticle diffusivity  $\mathcal{D}_p$  to free solution diffusivity  $\mathcal{D}_f$  as follows:

$$\mathcal{D}_p/\mathcal{D}_f = 1/\kappa K_D^{-1} \quad (1)$$

This parameter  $\mathcal{D}_p$  is the pore diffusivity that an observer in the pore would determine by measuring the root-mean-square distance a solute travels in a given time. This pore diffusivity is related to an “effective” diffusivity that an extraparticle observer would determine by measuring the solute flux into the particle and assuming Fick’s law without taking into account the surface area not accessible to the solute:

$$D_{\text{effective}} = \epsilon_p^* \mathcal{D}_p \quad (2)$$

Here,  $\epsilon_p^*$  is the effective void volume of the particle for the species of interest, and if  $\epsilon_p^*$  does not change as a function of the radial position in the particle,  $\epsilon_p^*$  is also the effective open particle area available for the solute.

Most work on proteins in chromatographic media has used either dynamic adsorption in a finite bath<sup>12–18</sup> or step response or pulse response techniques.<sup>19–27</sup> These dynamic methods are often confounded by other mass transport limitations such as boundary-layer mass transport, axial dispersion, or low adsorption rates, which are often accounted for with published correlations. Errors in these correlations project systematically onto the measurement of the intraparticle diffusion coefficient, casting doubt onto the validity and scope of the measurement. Other optical techniques require a slab geometry such as light scattering techniques or fluorescent recovery after photobleaching.<sup>28</sup> Some optical work has been done using interferometry in a single bead.<sup>29</sup> These optical techniques impose severe constraints on the geometry or refractive index of the chromatographic media and are not suitable for the vast majority of the chromatography particles used in industry.

This paper reports measurements of diffusivities of several proteins in nonadsorbing rigid-polymer and bonded-phase-silica chromatographic media using pulsed-field-gradient NMR (PFG-NMR) of both proton (<sup>1</sup>H) and fluorine (<sup>19</sup>F) nuclei. PFG-NMR avoids many of the ambiguities associated with transient intraparticle diffusion measurements such as dynamic adsorption

TABLE 1: Protein Stokes Radius,  $r_s$

protein	Stokes radius (Å)	mol wt by SEC (kDa)
F-ovalbumin, heavy labeling	41.7 ± 1.6	80
F-conalbumin	40.0 ± 2.0	80
F-ovalbumin, light labeling	33.6 ± 2.0	45
ovalbumin	33.6 ± 2.0	45
lysozyme	21.3 ± 2.0	14

TABLE 2: Pore Size,  $R_{\text{pore}}$

media	pore size (Å)
HW65	1000
HW55	300
Baker Bond PEI 300	208

<sup>†</sup> Present address: BioSeptra, 140 Locke Dr., Marlborough, MA 01752. Email: jcoffman@bioseptra.com.

<sup>⊗</sup> Abstract published in *Advance ACS Abstracts*, January 15, 1997.

in a finite bath and column pulse response experiments. A review of techniques and experimental errors<sup>30</sup> concluded that the PFG-NMR technique was the most precise and accurate method for determining intraparticle diffusivities. As PFG-NMR measurements do not depend on opacity, particle size, or particle shape, this technique is applicable to a wide variety of chromatographic systems: polymer, gel, and silica media, and systems with large particle size distributions.

PFG-NMR has been successfully used to measure intraparticle diffusivities that are not confounded by other mass transfer mechanisms. Gibbs et al.<sup>31</sup> measured the diffusion coefficient of fluorine-labeled ovalbumin with PFG-NMR in a polymeric size-exclusion media as a function of concentration. They found that the intraparticle diffusivity was well characterized by a factor  $\kappa K_D^{-1}$  of  $2.2 \pm 0.2$ .

PFG-NMR measures the intradiffusion coefficient,<sup>32,33</sup> also called the tracer-diffusion coefficient or (usually incorrectly) the self-diffusion coefficient. The relationship between the intradiffusion coefficient and the more common mutual (or interdiffusion) coefficient found in Fick's law has been discussed elsewhere.<sup>34–37</sup> The factor  $\kappa K_D^{-1}$  should be the same for both the intradiffusivity and mutual diffusivity,<sup>31</sup> since this factor depends on the physical geometry of the pore network and the hydrodynamic interaction between the protein and the pore.

Essentially, PFG-NMR magnetically tags each protein, allows it to diffuse for a chosen time, and then determines the distance traveled.<sup>32,33</sup> Time scales involved are on the order of 10 ms to 1 s, and length scales investigated are on the order of  $10^{-1}$   $\mu$ m to hundreds of micrometers. The technique measures diffusivities between  $10^{-4}$  and  $10^{-9}$  cm<sup>2</sup>/s.

The magnetic tags are imposed and decoded by applying a magnetic field gradient to the sample volume. The field-gradient intensity  $I_{gc}$ , duration  $\delta$ , and the diffusion time  $\Delta$  determine the length scale of displacement measured. The NMR signal is related to the diffusivity and the experimental parameters by

$$A = A_0 \exp[-(\gamma I_{gc} \delta)^2 D(\Delta - \delta/3)] \quad (3)$$

where  $A$  is the signal intensity,  $A_0$  is the signal intensity unattenuated by diffusive random motion,  $I$  is the current to the gradient coil, and  $g_c$  is the field gradient produced by the gradient coil per unit current in the coil. When there is a significant NMR background signal contribution from the chromatographic media, eq 3 is augmented by adding a constant. The fitted intensity of this nondiffusion contribution is required to be consistent with independent NMR measurements of the background contribution.

Since proton NMR signals detect all the protons in the sample, reduction or elimination of the confounding signals of the water, buffer, and chromatographic media is necessary. This can be done either by using proton PFG-NMR on an essentially deuterated system (solvent, buffer, and exchangeable protein protons converted to <sup>2</sup>H) and accounting for the residual polymer background, as discussed above, or by fluorine labeling proteins and using fluorine PFG-NMR. In both cases, signal from interstitial protein was removed by replacing interstitial aqueous solution with an organic solution. While the fluorine labeling denatures the protein as discussed below, the results from the fluorine-labeled protein and the unlabeled protein agree within experimental error when plotted against the ratio of protein size to pore size. The free solution intradiffusion coefficients were obtained for the proteins as a function of concentration, ranging from 10 to 200 mg/mL except where noted. In this range, the intradiffusivity varies linearly with concentration. This linear relationship for intradiffusion appears relatively unaffected by ionic strength, pH, and protein charge.<sup>36</sup> Values for the

intraparticle intradiffusion coefficients were related to the free solution intradiffusion coefficients by a single factor  $\kappa K_D^{-1}$  independent of concentration.

## 2. Experimental Methods

Chicken ovalbumin, grade V (#A5503), hen egg-white lysozyme (#L6876), and conalbumin grade I (#C0755) were obtained from Sigma Chemical Co. (St. Louis, MO). Concentrations were determined by UV absorbance at 280 nm. The fluorine-labeling reagent was *S*-ethyl trifluorothiolacetate (ETF) obtained from Lancaster (Windham Hill, NH). Dimethyl and dibutyl phthalate were obtained from Aldrich. Water used was distilled deionized water with conductivity of 18 M $\Omega$  (Interlake Continental). All other chemicals were chromatography grade. Chromatographic media used were Toso-Haas (Rohm and Haas Philadelphia, PA) TSK-HW65S and TSK-HW55S and Baker Bond PEI 300 (J. T. Baker Phillipsburg, NJ). TSK-HW65S and HW55S are methacrylate size-exclusion resins. The Baker Bond PEI 300 is a porous silica bonded with a weak anion-exchange resin (polyethylenimine). Ionic strength and pH were adjusted in the Baker Bond PEI 300 to eliminate protein adsorption.

**2.1. Protein Preparation for Proton PFG.** Proteins were dissolved to 100 mg/mL, dialyzed against 100 volumes of distilled, deionized H<sub>2</sub>O, and lyophilized. In bringing the protein sample back to atmospheric pressure, air was first passed through a  $-80$  °C vapor trap to minimize adsorption of ambient water vapor. The dried protein was reconstituted to 100 mg/mL with 99.9% D<sub>2</sub>O, and the labile protons on the protein and waters of hydration in the protein were allowed to exchange for at least 1 h. The sample was then similarly lyophilized. This process was repeated again, and the protein was stored at  $-20$  °C.

Deuterated buffer was prepared by using monobasic sodium phosphate, whose protons are all labile. An 80 mM solution at pH 4.45 was lyophilized, reconstituted diluting to 80 mM with 99.9% D<sub>2</sub>O, lyophilized again, and desiccated until needed.

**2.2. Protein Fluorine Labeling for Fluorine PFG.** The protein fluorine-labeling method was adapted from the procedures of Fanger and Harbury.<sup>38</sup> *S*-Ethyl trifluorothiolacetate (ETF) was added to a 100 mg/mL solution of ovalbumin or a 20 mg/mL solution of conalbumin, both dissolved in a 0.5 M Na<sub>2</sub>PO<sub>4</sub> (pH 8.5) buffer. Two separate labeling batches were produced for the ovalbumin experiments reported here. Excess ETF ( $>1000:1$ ) was added to the protein mixture and allowed to react with the protein for 1 h. NaOH (1 M) was constantly added to maintain the pH between 7.8 and 8.2. Roughly 4 mL of 1 M NaOH was needed for every milliliter of ETF added. The resulting solution was then passed through a 0.45  $\mu$ m filter. Desalting, buffer exchange (to a 80 mM Na<sub>2</sub>PO<sub>4</sub> buffer, pH 4.5), and reactant separation were performed by passing the fluorinated protein through a BioRad P6 desalting column or via dialysis. The fluorine-labeled protein was then concentrated to approximately 100 mg/mL by ultrafiltration in a 25 mm Amicon ultrafiltration cell. This stock solution was stored at 4 °C for not more than 2 weeks before use, or lyophilized and stored at  $-20$  °C. Upon reconstitution, no undissolved ovalbumin was evident, although the conalbumin samples had a small amount of undissolved material. In either case, the samples were centrifuged at 20000g for 2 min and then passed through a 0.45  $\mu$ m filter. The effects of the fluorine labeling on the protein hydrodynamics are discussed below.

**2.3. Gel Slurries.** Gel slurries were prepared by removing fines and washing with 50 volumes of Milli-Q water and then with 10–20 volumes of 80 mM Na<sub>2</sub>PO<sub>4</sub>. The majority of

interstitial buffer was removed by vacuum filtration. On the addition of ovalbumin solution to a dried sample of HW55, the concentration of ovalbumin in the interstices was higher than the stock solution, indicating some preferential exclusion of ovalbumin over that of water. The rest of the samples were prepared by adding protein to a sample pretreated with the solution buffer.

Interstitial aqueous protein solution was excluded<sup>31</sup> by forcing an immiscible organic mixture into the interstices by centrifugation. For the proton PFG work, toluene-*d*<sub>8</sub> and carbon tetrachloride were mixed to a density intermediate between that of the aqueous solution and that of the gel. For the fluorine labeling, a mixture of dimethyl phthalate and dibutyl phthalate was used. The amount of aqueous protein solution removed was about 36–39% of the total bed volume, in good agreement with the void volume of packed beds. This procedure was shown to remove intraparticle solution and confine the protein-containing aqueous phase to the particles.<sup>31</sup>

**2.4. Pulsed-Field-Gradient NMR.** The NMR experiments were performed with equipment described elsewhere<sup>31</sup> and were carried out at  $25 \pm 0.1$  °C. Diffusion experiments were performed with either the standard Stejskal-Tanner pulse sequence or the stimulated echo modification.<sup>39,40</sup> A train of five gradient pulses of identical strength, duration, and delay preceded each initial rf pulse to achieve a pseudosteady state in eddy currents induced by the changing current in the gradient coil. The fixed diffusion time was either 16.7 or 133.3 ms, and gradients of up to 150 G/cm were used. These diffusion times allowed diffusion on the order of 9000 and 30 000 Å, which is much larger than the pore size of the particles, but much smaller than the particle size. Thus the solutes effectively sampled the pore wall effectively 10–30 times, allowing an effective average of the pore diffusivity to be determined. Radio frequency pulse widths used for a 90° nutation angle were 5.5 μs for proton nuclei and 11 μs for fluorine nuclei. Pulse delays were 5 s for proton work and 1 s for fluorine work. To improve signal to noise, fluorine echos were collected with a narrow 2500 Hz filter width. The number of scans was between 200 and 1000 for proton PFG-NMR and 2000–7000 for fluorine PFG-NMR. Typically, 10–20 data points at varying gradient currents were taken for proton work and 5–10 data points were taken for the fluorine work. Signal to noise for individual points was typically 20:1 and ranged from 10:1 to 100:1. The diffusivities were obtained by a nonlinear, weighted, least-squares fit of the NMR signal to the varied parameters (eq 3). The data were weighted with respect to the signal to noise ratio. The 95% error bars shown in the diffusivity plots show the uncertainty obtained from the fit to eq 3.

### 3. Results and Discussion

Presented first are the measurements of water diffusing in silica- and polymer-based media (Baker Bond PEI 300 and HW65), to show the limiting behavior of small solutes diffusing in these media. Next presented are the measurements of the intradiffusion coefficient for two proteins in free solution and in three different media using proton PFG-NMR. Shown next are measurements of the intradiffusion coefficient in both free solution and in two media for two fluorine-labeled proteins using <sup>19</sup>F PFG-NMR. The measurements include the intraparticle diffusivity of essentially four distinct proteins in three different media. The results permit determining that the proton and fluorine PFG-NMR agree by properly accounting for the size of the proteins relative to the size of the pores in which they were diffusing.

**3.1. Water in TSK HW65.** Water in TSK HW65 has two distinct mobilities: the major species' diffusion coefficient is a

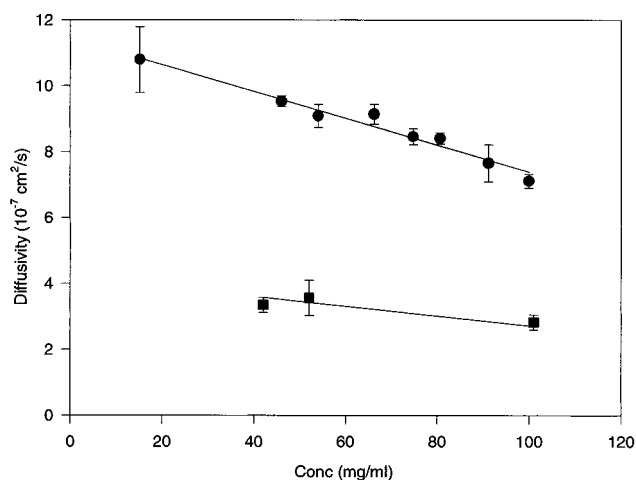


**Figure 1.** Free solution and intraparticle diffusivities of lysozyme in Baker Bond 300 using <sup>1</sup>H PFG-NMR.

factor of  $2.1 \pm 0.1$  lower than that in free solution ( $D_f = 2.29 \times 10^{-5}$  cm<sup>2</sup>/s); the minor species' is a factor of  $11 \pm 3$  lower than that in free solution. The first factor is consistent with a simple tortuosity effect, where a factor of 2 is expected for an isotropic porous medium. Any of several factors may explain the second, lower water mobility. The gel swells by more than a factor of 2 from its dry state on the addition of water, and the low diffusivity of water could be due to water associated with the gel matrix. Another possibility is that pores with size on the order of the water molecule (10 Å) are available to water and other low molecular weight molecules. The latter possibility is also consistent with preliminary diffusivity measurements of sodium fluoride and trifluoroacetate in these media, which also show a similar distribution of diffusivities. In either case, the sources of the lower water mobility component will not affect proteins significantly. The protein will not enter into 10 Å pores.

The background NMR signal associated with the matrix has a chemical shift near that of methyl groups, as expected for a methyl methacrylate resin. The background has a  $T_2$  of about 10 ms, near that of the protein, making a  $T_2$  separation of signals difficult. This background limits proton PFG diffusion measurements to above 50 mg/mL of protein.

**3.2. Water in Baker Bond PEI 300 Silica.** As in the case of the HW65, the water in the bonded phase silica exhibited two mobilities. The majority of the water signal in Baker Bond PEI 300 has a diffusion coefficient of  $(1.04 \pm 0.12) \times 10^{-5}$  cm<sup>2</sup>/s, a factor of 2.1 lower than that in free solution, while the remainder has a diffusion coefficient of  $(5.75 \pm 0.89) \times 10^{-7}$  cm<sup>2</sup>/s, a factor of 38 lower than that in free solution. The first factor can again be attributed to diffusion along a tortuous path. The lower water mobility is indicative of either water association with the PEI bonded phase or fine pores. Only the higher of the two diffusivities is important in understanding the pore networks and protein diffusion. A significant background signal comes from the bonded phase having magnitude and  $T_2$  similar to that of the HW65, which also limits concentrations studied to greater than 50 mg/mL for the proton PFG measurements.

**3.3. Lysozyme in Baker Bond PEI 300 Silica.** Shown in Figure 1 is a comparison of free solution and intraparticle diffusivities for native lysozyme in Baker Bond PEI 300 under nonadsorbing conditions. Each data point reports one proton PFG-NMR measurement at a particular concentration. The polymer background signal contributes significant spectral intensity, so the PFG-NMR data were fit to a model including the stationary background within the confidence intervals

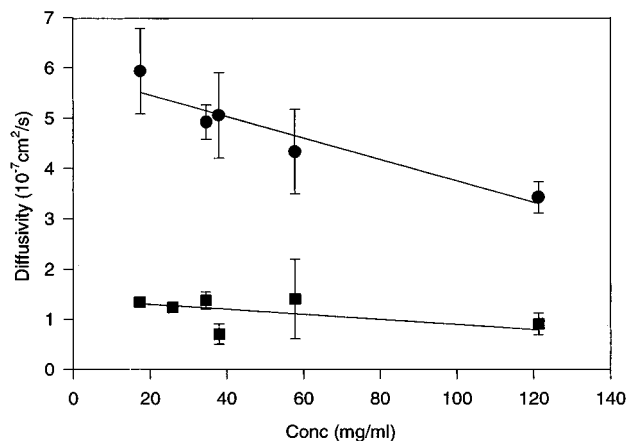


**Figure 2.** Free solution and intraparticle diffusivities of F-ovalbumin in HW55.

obtained from the protein-free experiment. The intraparticle diffusivity measured is significantly lower than the free solution diffusivity. As seen earlier for fluorine-labeled ovalbumin in TSK HW65,<sup>31,36</sup> both the free solution and intraparticle diffusivities are linear in concentration. The intraparticle diffusivities can be related to the free solution diffusivities by the factor  $\kappa K_D^{-1}$ , which is independent of concentration. Least-squares regression of the combined free solution diffusivity and intraparticle diffusivity data produces three parameters: the slope and intercept of the free solution diffusivity, and the factor  $\kappa K_D^{-1}$  to account for the decrease in intraparticle diffusivity relative to that in free solution. For lysozyme in free solution and in Baker Bond PEI 300,

$$\mathcal{D}_f = 11.3(\pm 0.20)[1 - 3.54(\pm 0.20)C] \quad (4)$$

$$\kappa K_D^{-1} = 2.72 \pm 0.11 \quad (5)$$

where the diffusivity is in  $10^{-7}$  cm<sup>2</sup>/s and the concentration is in g/mL.

The fit is shown as solid lines in Figure 1.

**3.4. Ovalbumin in HW55.** Only a single intraparticle diffusion coefficient of ovalbumin in HW55 at 300 mg/mL was obtained. The diffusivity measured was  $(3.74 \pm 0.17) \times 10^{-8}$  cm<sup>2</sup>/s, a factor  $\kappa K_D^{-1} = 3.3 \pm 0.3$  lower than that in free solution at the same concentration. The signal from the protein at this concentration was easily distinguishable from that of the water and the background.

**3.5. F-Ovalbumin in HW55.** Shown in Figure 2 are the free solution and intraparticle diffusivities for fluorine-labeled ovalbumin in TSK HW55 at several concentrations. The ratio of the free solution diffusivity to that in the particle is well described at all concentrations by a single factor. For F-ovalbumin in HW55,

$$\mathcal{D}_f = 5.88(\pm 0.24)[1 - 3.63(\pm 0.50)C] \quad (6)$$

$$\kappa K_D^{-1} = 4.2 \pm 0.5 \quad (7)$$

where the diffusivity is in  $10^{-7}$  cm<sup>2</sup>/s and the concentration is in g/mL. The fit is shown as solid lines in Figure 2. The slope of the free solution diffusivity is within experimental error of that for the unlabeled protein. In addition, using the Stokes volume of 1.11 mL/g<sup>36,41</sup> for ovalbumin, in the equations above, the slope with respect to volume fraction is  $3.3 \pm 0.5$ , which is within experimental error of the slope theoretically evaluated

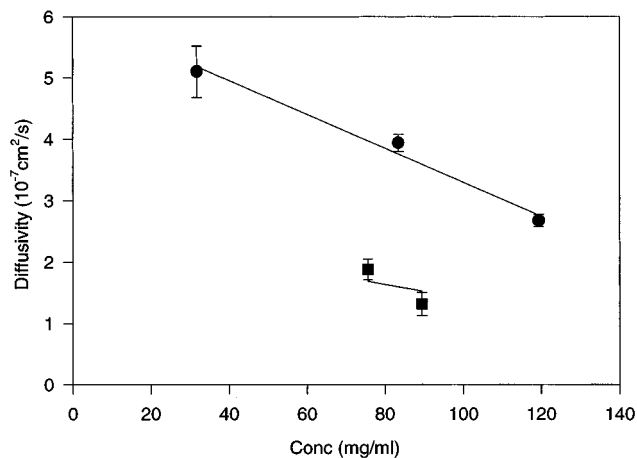


**Figure 3.** Free solution and intraparticle diffusivities of F-conalbumin in HW65.

by some researchers<sup>42,43</sup> for noninteracting hard spheres. It should be noted that the theoretically evaluated values of the slope  $A$  vary at least as much as the experimental error shown above.<sup>36</sup>

**3.6. F-Conalbumin in HW65.** Shown in Figure 3 are the results of measurements of the free solution and intraparticle diffusivities for fluorine-labeled conalbumin in TSK HW65 at two concentrations. The ratio of the free solution diffusivity to that in the particle is well described by a single factor. For F-conalbumin in HW65,

$$\mathcal{D}_f = 6.06(\pm 0.35)[1 - 4.55(\pm 0.44)C] \quad (8)$$

$$\kappa K_D^{-1} = 2.4 \pm 0.3 \quad (9)$$

where the diffusivity is in  $10^{-7}$  cm<sup>2</sup>/s and the concentrations in g/mL. The fit is shown as solid lines in Figure 3.

**3.7. Label Influence.** The effects of the fluorine-labeling procedure on ovalbumin used in this study were measured by size-exclusion chromatography (SEC), native PAGE, SDS-PAGE, and diffusivity measurements. SEC is sensitive to protein size, which can be correlated to protein molecular weight. SDS-PAGE with  $\beta$ -mercaptoethanol measures the molecular weight of proteins independent of native protein conformation by completely denaturing the protein and breaking disulfide bonds. Native PAGE measures qualitatively the size, conformation, and charge of the protein without denaturing them or breaking disulfide bonds. The infinite-dilution diffusion coefficient is related only to the conformation and size of the protein.

Size-exclusion chromatography, performed on a Waters Protein Pack 125, showed that the apparent molecular weight of the ovalbumin had increased from 45 to about 80 kDa. The SDS-PAGE was done with a PhastGel system (Pharmacia, Uppsala, Sweden). The results showed that the labeled protein was homogeneous and had a small molecular weight increase (less than 5 kDa). The native PAGE showed that the fluorine-labeled protein in its "native" form was homogenous and significantly more anionic than its unlabeled counterpart, as expected since ETF reacts primarily with the cationic lysine groups on the protein surface. The infinite-dilution diffusion coefficient, as measured by PFG-NMR, was lower than that of the unlabeled protein, indicating an increase in size.

The SEC measure of the molecular weight and the decrease in infinite-dilution diffusivity indicate that the labeled protein has assumed a larger configuration than the native protein. Since the SDS-PAGE did not show the same increase in molecular

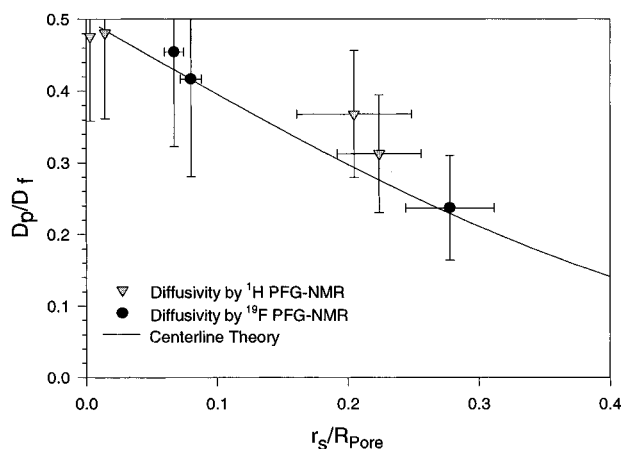


**Figure 4.** Effects of solute size and pore size on intraparticle diffusivity. The measured intraparticle diffusivity  $\mathcal{D}_p$  scaled by the free solution diffusivity  $\mathcal{D}_f$  is plotted versus the size of the solute Stokes radius,  $r_s$ , relative to that of the pore,  $R_{\text{pore}}$ . A comparison of the hydrodynamic interaction of the protein and the pore wall and that predicted for a hard sphere in a long cylinder is given by the line.<sup>44</sup>

weight, the increase in apparent molecular weight as seen by SEC cannot be explained by the weight of the fluorine tagging alone. A NMR spin count on the fluorine-labeled ovalbumin revealed 51 tags per molecule. These tags contribute 4500 g/mol to 48 500 MW. Therefore the decrease in diffusivity and the apparent increase in molecular weight as measured by SEC are due to denaturing of the ovalbumin by the labeling process.

These changes in protein conformation do not hinder the interpretation of the intraparticle diffusion measurements, but do indicate that the labeled protein is now a different probe. Heavy labeling cannot be considered a minor perturbation of the native protein, in contrast to the behavior seen for lightly labeled ovalbumin,<sup>31</sup> which showed only minor deviations from the behavior of the unlabeled protein. Protein–protein interactions in the heavily labeled ovalbumin are, however, similar to that in the unlabeled protein, as shown by the agreement between the slope of free solution diffusivity versus concentration and those reported for unlabeled ovalbumin.<sup>36</sup> These protein–protein interactions are related to the particle/pore interactions embodied in  $K_D$ . As indicated above, within experimental error and uncertainty in current theory, the heavily labeled protein behaves as a hard sphere as a function of volume fraction. Finally, the denaturing effect of heavy fluorine labeling is readily detected and quantified with any of the conformation-sensitive experimental probes discussed here. Thus any one measurement, such as free solution diffusion coefficients, will be adequate in future studies for describing the modified protein. These considerations permit the use of heavily labeled proteins to probe the intraparticle mobilities of proteins in general.

**3.8. Effect of Hindered Diffusion.** Figure 4 collects the intradiffusion coefficients for four proteins or variants (ovalbumin, fluorine-labeled ovalbumin, lysozyme, and fluorine-labeled conalbumin) and for water in three chromatographic media (HW65, HW55, and Baker Bond PEI 300) in reduced units. The Stokes radius,  $r_s$ , was calculated from the infinite-dilution diffusion coefficient,  $\mathcal{D}_0$ , for each protein:

$$\mathcal{D}_0 = kT/6\pi r_s \mu \quad (10)$$

where  $k$  is Boltzmann's constant,  $T$  is temperature, and  $\mu$  is solvent viscosity. This radius effectively treats each protein as a hard sphere of equivalent mobility. Equation 10 can be considered a definition of the Stokes radius. The pore radii

were taken from the manufacturer's literature for the HW65 and the bonded silica and were deduced from the reported exclusion limits for the HW55 by comparison with those found in silicas.

These pore radii are widely reported and in many cases provide the only available measurement of pore size for many chromatographic media users. The inaccuracy of these pore radii would result in scatter of the data horizontally in Figure 4. Estimates of the effect of the possible error inherent in these pore radii are shown in Figure 4. The estimate of errors obtained with first-order error propagation produced the horizontal error bars shown in Figure 4. The errors from the measurement of  $1/\kappa K_D^{-1}$  described above are also shown in the vertical error bars. In the limit of  $\lambda \rightarrow 0$  (small solutes or large pores), the value of  $K_D^{-1} \rightarrow 1$  and the value of  $1/\kappa K_D^{-1}$  becomes  $1/\kappa$ . Extrapolating to  $\lambda = 0$ , the tortuosity factor  $\kappa = 2.0 \pm 0.1$ , a value in agreement with that predicted by Epstein for an isotropic porous medium.<sup>3</sup> The dependence of  $1/\kappa K_D^{-1}$  on  $r_s/R_{\text{pore}}$  is due to the hydrodynamic interaction of the protein with the pore walls,  $K_D^{-1}$ . Shown for comparison is the prediction from the semiempirical correlation by Anderson and Quinn<sup>44</sup> for  $K_D$  for diffusion of a sphere in the center of a long cylinder, valid for  $\lambda < 0.4$ :

$$K_D = 1 - 2.1044\lambda + 2.089\lambda^3 - 0.948\lambda^5 \quad (11)$$

The data and the idealized model show agreement to within experimental error. The agreement of the Anderson–Quinn model for the diffusivity of several proteins in several kinds of chromatographic media is surprising, since the proteins are neither hard spheres nor are they restricted to the center of the pore, and the pores are not long cylinders with a single radius. The consistency of the intraparticle diffusivity measurements between the polymeric media and the silica media is also surprising, since there is no reason, *a priori*, to expect the pore networks to affect the mobility in the same manner. This agreement does suggest, however, that with unambiguous measurements of intraparticle diffusivity, broadly applicable correlations can be developed that relate intraparticle diffusivity to easily characterizable parameters such as protein size and pore size.

#### 4. Summary

PFG-NMR is an excellent and widely applicable technique for measuring protein diffusion coefficients in porous chromatographic media. Both proton and fluorine PFG-NMR can be used to determine these coefficients. The proton NMR needed higher protein concentrations to perform the experiments. The fluorine approach is less difficult experimentally, but high levels of labeling may produce some denaturation of the protein, and its subsequent effects on the protein structure and mobility must be considered.

Protein intradiffusion coefficients for each protein and variant examined decrease linearly with concentration in both free solution and porous media over the range 0–300 mg/mL. In a range of protein/pore sizes ( $0 < \lambda < 0.3$ ) the effects of the pore network on intraparticle diffusivity can be accounted for by separately characterized tortuosity ( $\kappa$ ) and hydrodynamic effects ( $K_D$ ). For four proteins or protein variants in three different chromatographic media, the results were well represented with a tortuosity factor,  $\kappa = 2.0 \pm 0.1$ , theoretically valid for isotropic porous media, in combination with additional attenuation of mobility  $K_D$  in accordance with that predicted for a sphere in a long cylinder.

**Acknowledgment.** The authors wish to acknowledge Tracy Peters for labeling work, the National Science Foundation for the grant (9204436) supporting this research, the Shell Corporation for the NMR Spectrometer used in this work, and the Upjohn Fellowship (J.L.C.).

## References and Notes

- (1) Lewellen, P. C. Hydrodynamic Analysis of Microporous Mass Transport. Ph.D. Thesis, University of Wisconsin, Madison, 1982.
- (2) Deen, W. M. *AIChE J.* **1987**, *33* (9), 409–1423.
- (3) Epstein, N. *Chem. Eng. Sci.* **1988**, *44* (3), 777–779.
- (4) Johnson, C. S. Academic Press: New York, 1965; Vol. 1, pp 33–102.
- (5) Satterfield, C. N.; Cadle, P. J. *Ind. Eng. Chem. Process Des. Dev.* **1968**, *7*(2):256–260.
- (6) Satterfield, C. N.; Cadel, P. J. *Ind. Eng. Chem. Fundam.* **1968**, *7*(2): 202–210.
- (7) Brown, L. F.; Haynes, H. W.; Manogue, W. H. *J. Catal.* **1969**, *14*, 220–225.
- (8) Satterfield, C. N. *Mass Transfer in Heterogeneous Catalysis*; MIT Press: Cambridge, 1970; pp 33–41.
- (9) Satterfield, C. N.; Colton, C. K.; Pitcher, W. H., Jr. *AIChE J.* **1973**, *19*(3):628–635.
- (10) Feng, C.; Stewart, W. E. *Ind. Eng. Chem. Fundam.* **1973**, *12*(2): 143–147.
- (11) Haynes, H. W.; Brown, L. F. *AIChE J.* **1971**, *17*(2):491–494.
- (12) Colton, C. K.; Satterfield, C. N.; Lai, C. J. *AIChE J.* **1973**, *19*(3): 628–635.
- (13) Arve, B. H.; Liapis, A. I. *AIChE J.* **1987**, *33*(2):179–193.
- (14) Graham, E. E.; Dranoff, J. S. *Ind. Eng. Chem.* **1982**, *21*:360–365.
- (15) Tsou, H. S.; Graham, E. E. *AIChE J.* **1985**, *31*(12):1959–1966.
- (16) Pinto, N. G.; Graham, E. E. *React. Polym.* **1987**, *5*:49–53.
- (17) McCoy, M. A.; Liapis, A. I. *J. Chromatogr.* **1991**, *548*:25–60.
- (18) Chase, H. A. *Chem. Eng. Sci.* **1984**, *39*(7/8):1099–1125.
- (19) Walters, R. R. *J. Chromatogr.* **1982**, *249*:19–28.
- (20) Arnold, F. H.; Blanch, H. W.; Wilke, C. R. *Chem. Eng. J.* **1985**, *30*:B9–B36.
- (21) Arnold, F. H.; Blanch, H. W.; Wilke, C. R. *Chem. Eng. J.* **1985**, *30*:B25–B36.
- (22) Arnold, F. H.; Schofield, S. A.; Blanch, H. W. *J. Chromatogr.* **1986**, *355*:1–12.
- (23) Arnold, F. H.; Schofield, S. A.; Blanch, H. W. *J. Chromatogr.* **1986**, *355*:13–27.
- (24) Gibbs, S. J.; Lightfoot, E. N. *Ind. Eng. Chem. Fundam.* **1986**, *25*, 490–498.
- (25) Boyer, P. M.; Hsu, J. T. *AIChE J.* **1992**, *38*(2):259–272.
- (26) Ghrist, F. D.; Stadalius, M. A.; Snyder, L. R. *J. Chromatogr.* **1987**, *387*, 1–19.
- (27) Ghrist, F. D.; Stadalius, M. A.; Snyder, L. R. *J. Chromatogr.* **1987**, *387*, 20.
- (28) Berk, D. A.; Yuan, F.; Leunig, M.; Jain, R. K. *BIOPHYS J.* **1993**, *65*:2428–2436.
- (29) Korthäuer, W.; Gelleri, B.; Sernetz, M. *Ann. N.Y. Acad. Sci.* **1987**, *501*:517–521.
- (30) Westrin, B. A. Ph.D. Thesis, Department of Chemical Engineering I, Lund, Sweden, 1991.
- (31) Gibbs, S. J.; Lightfoot, E. N.; Root, T. W. *J. Phys. Chem.* **1992**, *96*:7458–7462.
- (32) Stilbs, P. *Prog. NMR Spectrosc.* **1987**, *19*:1–45.
- (33) Kärger, J.; Pfeifer, H.; Heink, W. *Adv. Magn. Reson.* **1988**, *12*: 1–89.
- (34) Albright, J. G.; Mills, R. *J. Phys. Chem.* **1965**, *69*(9):3120–3126.
- (35) Tyrrell, H. J. V.; Harris, K. R. *Diffusion in Liquids*; Butterworths: Boston, 1984.
- (36) Gibbs, S. J.; Chu, A. C.; Lightfoot, E. N.; Root, T. W. *J. Phys. Chem.* **1991**, *95*:467–471.
- (37) Gibbs, S. J. Protein Diffusion and Chromatography. Ph.D. Thesis, UW–Madison, 1989.
- (38) Fanger, M. W.; Harbury, H. A. *Biochemistry* **1965**, *4*:2541–2545.
- (39) Stejskal, E. O.; J. E. *J. Chem. Phys.* **1965**, *42*(1):288–292.
- (40) Tanner, J. E.; Stejskal, E. O. *J. Chem. Phys.* **1968**, *49*(4):1768–1777.
- (41) Jeffrey, P. D.; Nichol, L. W.; Turner, D. R.; Winzor, D. J. *J. Phys. Chem.* **1977**, *81*(8):776–781.
- (42) Pusey, P. N.; Tough, R. J. A. *Particle Interactions*; Plenum Press: New York, 1985; pp 85–179.
- (43) Kops-Werkhoven, M. M.; Fijnaut, H. M. *J. Chem. Phys.* **1982**, *77*(5):2242–2253.
- (44) Anderson, J. L.; Quinn, J. A. *Biophys. J.* **1974**, *14*:130.